Journal of Thermal Science Vol.28, No.1 (2019) 97−105

https://doi.org/10.1007/s11630-018-1059-3 **Article ID: 1003-2169(2019)01-0097-09**

Influence of Solids Circulation Flux on Coal Gasification Process in a Pressurized High-density Circulating Fluidized Bed

ZHANG Yawen[1,2,3], LEI Fulin[2,3] *, XIAO Yunhan[2,3]

1. Collaborative Innovation Center of Chemical Science and Engineering (Tianjin), School of Chemical Engineering and Technology, Tianjin University, Tianjin 300072, China
2. Key Laboratory of Advanced Energy and Power, Institute of Engineering Thermophysics, Chinese Academy of Sciences, Beijing 100190, China
3. University of Chinese Academy of Sciences, Beijing 100049, China

Abstract: The coal gasification behaviors in the pressurized high-density circulating fluidized bed under various solids circulation fluxes were studied with the CFD method, which combines the two-fluid model and coal gasification reactions represented by the chemical percolation devolatilization and the MGAS models. The numerical method was validated with two experimental cases, and detailed distributions of gas species and temperature in the riser were illustrated to understand the gasification process. To fully understand the influence of solids circulation flux on the gasification behavior, a series of cases were simulated with the solids flux varying gradually from 260 to 1010 kg/m^{2}s, and the composition and quality of syngas were compared between various cases. The higher heating value of syngas firstly increased and then decreased with the increase of solids flux, and it reached the highest value around 480 kg/m^{2}s. The influence of solids flux on gasification process was further analyzed through the contours of temperature, solids concentration, and gas composition in the riser.

Keywords: CFD, two-fluid model, gasification, high-density CFB

1. Introduction

Coal is widely distributed around the world and will continue to be the most important part in the energy market especially in China [1]. The combustion process accounts for most of coal consumption, which releases a large amount of SO_x, NO_x and CO_2, thus it is important to develop clean coal technology [2]. The gasification technology that converts coal into combustive syngas mainly including CO and H_2 has been widely accepted as a promising choice to utilize coal cleanly [3, 4]. In the industrial practices, several gasification technologies such as entrained bed, low-density and high-density circulating fluidized bed (CFB) are applied.

The main advantages of the entrained bed gasifier include its higher coal conversion rate and stronger turbulence mixing between coal and gaseous mixture [5]. However, it is operated under high temperature and needs large amount of oxygen, which makes the entrained bed gasifier challenging to be designed and operated [6]. The CFB gasifier is operated under lower temperature (usually below 1000°C), which can effectively decrease the cost [7]. Up to now, the CFB gasifier is usually operated under low solids circulation rate (e.g., G_s < 100 kg/m^{2}s)

Received: July 19, 2018 Corresponding author: LEI Fulin E-mail: leifulin @iet.cn

Nomenclature

Symbols

d_s	Particle diameter/m	T_g	Temperature of the gas phase/K
D_{O_2}	Oxygen diffusivity/$cm^2 \cdot s^{-1}$	T_s	Temperature of solids phase/K
k_a	Ash-layer diffusion rate constant /$g \cdot cm^{-2} \cdot atm^{-1} \cdot s^{-1}$	X_i	Mass fraction of species i
k_f	Film diffusion rate constant/$g \cdot cm^{-2} \cdot atm^{-1} \cdot s^{-1}$	X_i^0	Initial value of X_i
k_r	Kinetic rate constant/$g \cdot cm^{-2} \cdot atm^{-1} \cdot s^{-1}$	**Greek letters**	
M_i	Molecular weight of species i	ε_g	Volume fraction of the gas phase
P_i	Partial pressure of species i/atm	ε_s	Volume fraction of the solids phase
R	Universal gas constant/$cal \cdot mol^{-1} \cdot K^{-1}$	μ_g	Viscosity of the gas phase/$g \cdot cm^{-1} \cdot s^{-1}$
R_{O_2}	Gas constant for oxygen/$atm \cdot cm^3 \cdot g^{-1} \cdot K^{-1}$	ρ_g	Density of the gas phase/$g \cdot cm^{-3}$
r_n	Rate of reaction n/$mol \cdot cm^{-3} \cdot s^{-1}$	ρ_s	Density of the solids phase/$g \cdot cm^{-3}$

and ambient pressure [8, 9]. The pressurized high-density CFB gasifier is operated under higher solids circulation flux, higher pressure, similar low temperature [10, 11] with the low-density CFB gasifier, and it has great potential due to its large unit capacity and easy to scale up. However, the pressurized gasification process under high solids circulation flux is lack of understanding [12, 13], and it needs to be further studied with experimental and numerical methods. It is difficult to fully describe the pressurized gasification process in the laboratory, and it is essential to develop numerical methods such as the CFD modelling.

The CFD simulation can provide detailed information about hydrodynamics characteristics, distributions of temperature and species concentration, thus it has been employed to investigate the gasification and combustion behavior in various fluidized beds [14, 15]. There are two approaches to describe the gas-solid hydrodynamics, namely, Eulerian-Lagrangian [16, 17] and Eulerian-Eulerian method [10, 18-20]. The Eulerian-Eulerian two-fluid model is popular in simulating the gas-solid behavior of the low-density CFB [21, 22] and the high-density CFB [10, 23, 24]. Some researchers have simulated coal gasification process based on two-fluid model, and these studies mainly focus on the bubbling fluidized bed (BFB) gasifier (such as Yu et al. [25], Wang et al. [26] and Armstrong et al. [27, 28]). Recently, Zhang et al. [29] developed a two-dimensional model to predict the gasification process in a low-density CFB riser. These studies reveal that the Eulerian-Eulerian model coupled with suitable chemical reaction model can be a good way to simulate the gasification behavior in the BFB (Bubbling Fluidized Bed) and CFB gasifier. However, there are few numerical studies on the pressurized gasification process in the high-density CFB riser, which needs a suitable CFD method.

The high-density CFB is characterized with high solids circulation flux, and some researchers have focused on the effects of solids circulation flux on the gas-solid flow behaviors in the lab-scale high-density CFB. Xiao et al [30] investigated the hydrodynamics characteristics under various solids circulating fluxes in the lab-scale cold high-density circulating fluidized bed. Wang et al. [31, 32] systematically investigated axial and radial profiles of solids concentration and velocity under high solids circulation flux (up to 1000 kg/m^2s) in a high-density CFB riser for FCC (Fluid Catalytic Cracking) particles. Chang et al. [33] studied the effects of solids circulation flux on the gas-solid flow behaviors in a high-density CFB riser for Geldart B particles. These studies reveal that axial and radial profiles of solids concentration change a lot under different solids circulation fluxes. The gasification process is a combination of gas-solid hydrodynamics, chemical reaction, heat and mass transfer processes. The gas-solid flow behavior will affect the heat and mass transfer process, the gasification reactions, as well as the gasifier operation. However, there is rare literature on how the solids circulation flux influences the gasification process, since it is difficult to get detailed information of gasification process with experimental methods. The CFD method can give more details of gasification process, and it is more convenient to study the effects of solids circulation flux, which can help us operate the high-density CFB gasifier more effectively.

In this work, the CFD method for pressurized high-density CFB gasifier is developed under the framework of two-fluid model. The kinetic rate of char-steam gasification rate is determined through the sensitivity analysis. The developed numerical method is validated with two experimental cases. The validated CFD method is then employed to investigate how the solids circulation flux affects the flow behavior and the gasification performance in a wide range for the high-density CFB.

2. Experimental setup

The coal gasification experiments were performed in a lab-scale pressurized high-density CFB, whose schematic diagram is shown in Fig. 1(a). The riser is 0.102 m diameter and 17.0 m high from the solid-inlet. Silicon sand was used as the bed material, and all sand particles were initially packed in the J-leg and the standpipe on the start of gasification experiment. The lignite coal was transported into the riser from the coal-inlet, and Table 1 provides the coal properties. The gas mixture including air, oxygen and steam was introduced into the riser through the gas-inlet at the bottom of the riser. The gasification processes are operated around 0.6 MPa, and the detailed operating conditions and gasification results are listed in Table 2. In this work, only the riser is simulated, and the two-dimensional model is used as shown in Fig. 1(b), which is selected based on the previous work of our group on the simulation of gas-solid flow behavior in this system.

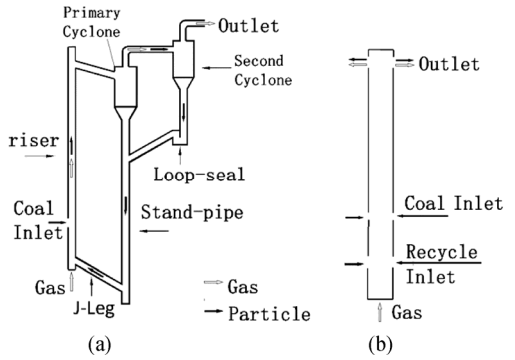

Fig. 1 Schematic diagrams of (a) the HDCFB and (b) the riser used in the simulations

Table 1 Properties of coal and bed material

Physical properties	Value
Coal proximate analysis (*wt*%, *ad*)	
Fixed carbon	49.86
Volatile matter	28.27
Moisture	10.81
Ash	11.06
Coal ultimate analysis (*wt*%, *daf*)	
Carbon	77.76
Hydrogen	4.32
Oxygen	16.26
Nitrogen	1.09
Sulfur	0.57
Higher heating value/MJ·kg^{-1}	21.46
Bed material properties	
Mean particle size/mm	0.137
Apparent density/kg·m^{-3}	2568
Packed density/kg·m^{-3}	1609

Table 2 Operating conditions and experiment results

Case	1	2
Coal feed flow rate/kg·h^{-1}	137.67	123.8
Air supply flow rate/kg·h^{-1}	308	355
Oxygen supply/kg·h^{-1}	35.4	33.9
Operating pressure/bar	6.06	6.2
Temperature of reactor/K	1117	1117
Pressure drop/kPa	8.85	8.60
Measured gas composition/% (mole fraction)		
CO	13.18	11.16
CO_2	15.84	16.31
H_2	6.59	5.11
CH_4	1.75	1.16
N_2	62.09	65.72

3. Numerical method

3.1 Governing equations

The two-fluid model is applied to describe the hydrodynamics of the riser, and its governing equations can be found in our previous work [10]. Besides the hydrodynamics, the gasification process also involves heat transfer and chemical reaction, thus it is essential to solve the conservation equations of energy and species transport. In this work, the gas-solids interphase heat transfer is modelled with Gunn equation [34], while the heat transfer between solids is neglected.

3.2 Chemical reaction model

Coal is divided into four compositions as char (FC), volatile matter (VM), moisture (M) and ash. The gas phase in the gasifier mainly consists of 11 species (CO, CO_2, H_2O, H_2, O_2, N_2, H_2S, NH_3, Tar, CH_4 and C_2H_2). In this work, we assume char as pure carbon without other contents. Table 1 displays the proximate and ultimate analysis of the coal. We derive the equivalent formula of volatile matter as $C_{1.985}H_{6.845}O_{1.245}N_{0.1036}S_{0.121}$. The coal gasification process mainly includes pyrolysis, heterogeneous and homogeneous reactions.

Coal is firstly dried after being heated in the gasifier. The rate of coal drying is based on the METC Gasifier Advanced Simulation (MGAS) model [35].

$$\text{Moisture (coal)} \rightarrow H_2O \qquad \text{(R1)}$$

$$r_1 = 1.1\times10^5 \exp\left(-21200/RT_s\right)\varepsilon_s\rho_s X_M \qquad (1)$$

In this work, the Chemical Percolation Devolatilization (CPD) model [36] is used for the modeling of pyrolysis process. The six-parameter two-stage model from the Carbonaceous Chemistry for Computational Modeling (C3M) software is applied to model the pyrolysis rate. The composition of released gases is calculated with the modified-CPD model and the

details are described in our previous work [29].

Volatile Matter $\rightarrow \alpha_1 CO+\alpha_2 CO_2+\alpha_3 CH_4+\alpha_4 H_2O+\alpha_5 Tar+\alpha_6 C_2H_2+\alpha_7 H_2+\alpha_8 H_2S+\alpha_9 NH_3$ (R2)

$$r_2 = \left(2.71\times10^6 \exp\left(-26968/RT_s\right) + 593.51\exp\left(-15412.5/RT_s\right)\right)\varepsilon_s\rho_s\left(X_{VM}-X^*\right) \quad (2)$$

The heterogeneous reactions involved in the gasifier are char combustion and gasification reactions. The rates of heterogeneous reactions such as char combustion, CO_2 gasification and methanation used in this work are based on the MGAS model.

$$2C + O_2 \rightarrow 2CO \quad (R3)$$

$$r_3 = 6\varepsilon_s P_{O_2} \Big/ \left[d_s\left(1/k_f + 1/k_a + 1/k_r\right)\right] \quad (3)$$

$$C + CO_2 \leftrightarrow 2CO \quad (R4)$$

$$r_4 = 2250\exp\left(-42000/RT_g\right)\left(P_{CO_2} - P_{CO}^2\Big/\left(\exp\left(20.92-20282/T_g\right)\right)\right)\left(\varepsilon_s\rho_s X_{FC}/M_{FC}\right) \quad (4)$$

$$C + 2H_2 \leftrightarrow CH_4 \quad (R5)$$

$$r_5 = \exp\left(-7.087-8078/T_g\right)\left(P_{H_2} - \sqrt{P_{CH_4}\Big/\exp\left(-13.43+10999/T_g\right)}\right)\left(\varepsilon_s\rho_s X_{FC}/M_{FC}\right) \quad (5)$$

The char-steam gasification reaction rate is based on the MGAS model and determined by the sensitivity analysis as described in the following section.

$$C + H_2O \leftrightarrow CO + H_2 \quad (R6)$$

$$r_6 = 8.0\times10^5\exp\left(-42000/RT_g\right)\left(P_{H_2O} - P_{H_2}P_{CO}\Big/\exp\left(17.29-16326/T_g\right)\right)\left(\varepsilon_s\rho_s X_{FC}/M_{FC}\right) \quad (6)$$

The homogeneous reactions involved during the gasification process are mainly the gaseous combustion reactions and water-gas shift reaction. The kinetic rates of these reactions are taken from MGAS model, where the symbol [ ] represents the species mole concentration, e.g., [CO].

$$CO + 0.5O_2 \rightarrow CO_2 \quad (R7)$$

$$r_7 = 3.98\times10^{14}\ \exp\left(-40000/RT_g\right)\varepsilon_g\left[O_2\right]^{0.25}\left[H_2O\right]^{0.5}\left[CO\right] \quad (7)$$

$$H_2 + 0.5O_2 \rightarrow H_2O \quad (R8)$$

$$r_8 = 1.0\times10^{16}\exp\left(-30000/RT_g\right)\varepsilon_g\left[O_2\right]\left[H_2\right] \quad (8)$$

$$CH_4 + 2O_2 \rightarrow CO_2 + 2H_2O \quad (R9)$$

$$r_9 = 6.7\times10^{12}\exp\left(-48400/RT_g\right)\varepsilon_g\left[O_2\right]^{1.3}\left[CH_4\right]^{0.2} \quad (9)$$

$$CO + H_2O \leftrightarrow CO_2 + H_2 \quad (R10)$$

$$r_{10} = 2.877\times10^5 f\exp\left(-27760/RT_g\right)\left(P_{CO}P_{H_2O}/P^2 - P_{CO_2}P_{H_2}/P^2K_{eq}\right)P_{atm}^{\left(0.5-\left(P_{atm}/250\right)\right)} \quad (10)$$

$$f = 0.068\varepsilon_g\left(1-\varepsilon_g\right)\rho_s X_{Ash}\exp\left(-8.91+5553/T_g\right) \quad (11)$$

$$K_{eq} = \exp\left(-3.63061+3955.71/T_g\right) \quad (12)$$

$$Tar + 13.59O_2 \rightarrow 10.8CO_2 + 5.76H_2O \quad (R11)$$

$$r_{11} = 3.8\times10^{11}\exp\left(-30000/RT_g\right)\varepsilon_g\left[O_2\right]^{1.5}\left[Tar\right]^{0.25} \quad (13)$$

$$Tar \rightarrow 7.74C + 0.18CO + 2.88CH_4 \quad (R12)$$

$$r_{12} = 2.5\times10^7\exp\left(-29000/RT_g\right)\varepsilon_g\left[Tar\right] \quad (14)$$

3.3 Simulation setup

The governing equations are solved with the ANSYS Fluent 13.0, and the chemical reaction model is implemented in a user defined function (UDF). Two solid phases (coal and sand) are included in the system, and Table 2 provides the operating conditions of coal gasification experiments. The coupled differential equations are solved by the Phase Coupled SIMPLE algorithm. The time step is set as 5×10^{-4} s and the simulation lasts 80 s to get a quasi-steady state. The steady simulation results are time-averaged from 60 to 80 s. The solids volume fraction for sand is set as 0.035 based on the experimental data of pressure drop. The temperatures of all phases are initially set the same with the operating temperature of the gasifier. The mass flow rate and compositions of sand and coal out of the riser are calculated with a UDF, and the simulation of downer is avoided. And then the solid recycle inlet boundary conditions are set based on these calculations. The no-slip and the partial slip wall boundary conditions are set for gas phase and solid phase, respectively. The specularity coefficient is 0.005 based on hydrodynamics study of the riser of high-density circulating fluidized bed [10]. The radiation heat transfer from the wall to the surroundings is dominant in the heat loss, and the radiation wall condition is employed in this study. The mesh independent study has been done to choose an appropriate grid size, and the two-dimensional grid with 12×1400 cells is used in this work.

3.4 Sensitivity analysis of char-steam reaction rate

The pre-exponential factor for char-steam gasification from MGAS model was 2.25×10^3 $atm^{-1}s^{-1}$, but the predicted mole fraction of CO and H_2 was much lower than the experimental data. Other researchers [2, 29, 37] also found that the MGAS model under-predicted mole fraction of CO and H_2 resulting from the lower char-steam gasification rate. In this work, a parametric study for this reaction has been performed, and the pre-exponential factor is varied as 2.25×10^3, 2.25×10^4, 2.25×10^5 and 8.00×10^5 $atm^{-1}s^{-1}$. Fig. 2 displays the predictions of mole fraction for CO and H_2 with different pre-exponential factors. The predicted mole fraction of CO and H_2 increases dramatically as this reaction accelerates. To get a better predicted result, the pre-exponential factor is selected as 8.00×10^5 $atm^{-1}s^{-1}$ in this work.

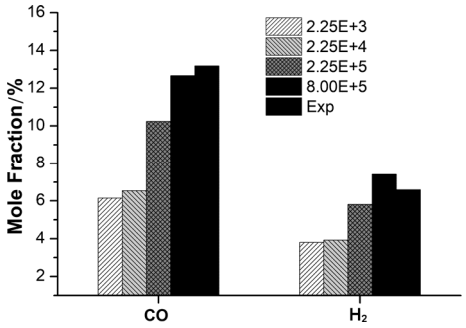

Fig. 2 The predicted mole fraction of CO and H_2 out of the riser with different pre-exponential factors for char-steam reaction

4. Results and discussion

4.1 Model validation

Fig. 3 displays the transient mole fractions of syngas out of the riser over 80 s period. It can be seen that the simulation has arrived at a quasi-steady state from 40 s. In this study, the time-averaged results are calculated between 60 s and 80 s. Fig. 4 shows comparisons of the gas mole fraction out of the riser between predicted results and experimental data for Case 1 and Case 2. The predicted results of syngas composition for Case 1 and Case 2 are in good agreement with the experimental results, which indicates that the numerical method is able to predict the coal gasification process reasonably.

Fig. 5 displays contours of predicted mass fractions and temperature of gaseous species across the riser for Case 1. It can be seen that oxygen is mainly consumed in the lower part of the riser especially near the solids recycle inlet. As the unreacted char is recycled into the riser, the char-combustion reaction takes place quickly in this region, and much carbon-monoxide is produced. The produced carbon-monoxide mainly accumulates near the wall due to higher solids concentration. The produced carbon-monoxide is further combusted with the excess oxygen and a large amount of carbon-dioxide is produced.

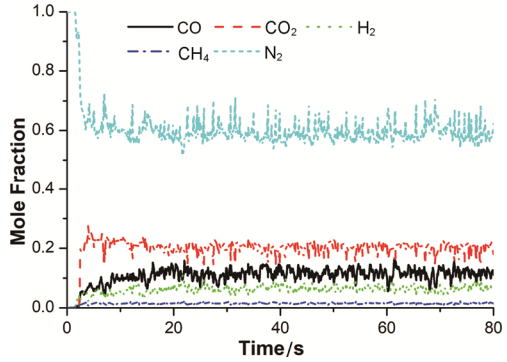

Fig. 3 The transient mole fractions of syngas out of the riser over 80 s period for Case 1

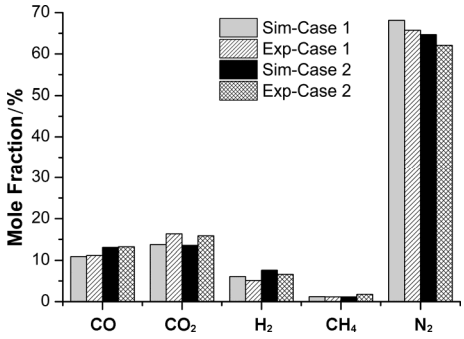

Fig. 4 Comparisons of the gas mole fraction out of the riser between model predictions and experimental data

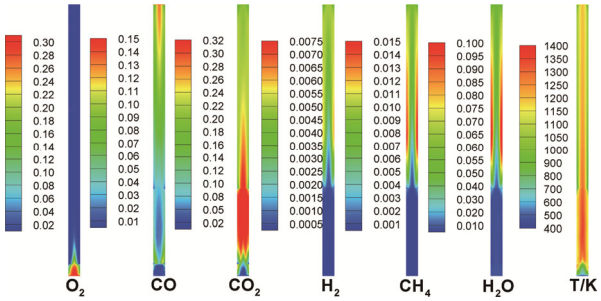

Fig. 5 Contours of predicted mass fractions and temperature of gaseous species in the riser for Case 1

As coal enters the riser through the coal-inlet, it is quickly heated, and the water and volatile matter in the coal is then immediately released. The mass fraction of H_2O has an obvious increase near the coal-inlet. The mass fraction of carbon-dioxide begins to decrease while the mass fraction of carbon-monoxide increases near the coal-inlet due to the char-CO_2 gasification reaction. In the upper part of the riser, the mass fractions of carbon-monoxide and hydrogen make a dramatic increase due to the char-steam gasification reaction. Below the coal-inlet, the combustion reactions are dominated until oxygen are exhausted, thus the temperature has a dramatic increase in this region as shown in the contour of gas temperature. Above the coal-inlet, the temperature begins to descend near the coal-inlet, because the coal drying, coal pyrolysis and char gasification reactions are all endothermic reactions. The above analysis reveals that the riser can be divided into combustion zone below the coal-inlet and the gasification zone above the coal-inlet.

To further illustrate the gasification process in the riser, Fig. 6 displays the predicted mass flow rates for different species along the riser for Case 1. It can be seen that the oxygen is almost completely consumed at the height of 4 m, and the mass flow rates of CO and CO_2 increase dramatically below 4 m. In this region, the amount of H_2O is almost kept constant and little H_2 and CH_4 is

produced, which also reveals that the char-combustion reaction is dominant in this region. Above the height of 4.0 m, the char-CO_2 gasification reaction results in an increase of carbon monoxide. From the height of 8.0 m, char reacts with both H_2O and CO_2, which leads to the rise of CO and H_2 and the fall of CO_2 and H_2O. The vertical line represents the mass flowrates calculated based on the formula of pyrolysis process. It can be seen that most methane and about 30% hydrogen are released from pyrolysis process.

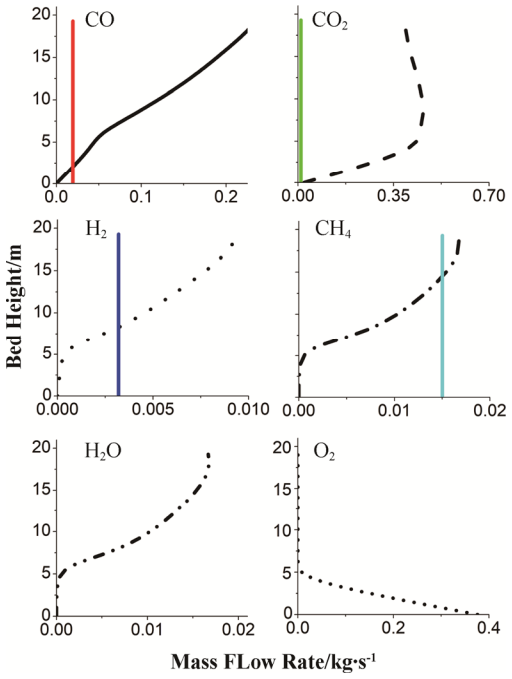

Fig. 6 The predicted gas mass flow rates for different species along the height of the riser for Case 1

4.2 Influence of solids circulation flux

The solids circulation flux has obvious effect on the flow hydrodynamics in the riser, which can provide different environment for chemical reactions in the gasifier. To study the effect of solids flux on the gasification performances in the riser, the initial volume fraction of bed material is varied, and other input parameters are set the same as Case 1 listed in Table 2. The solids circulation flux discussed in this section refers to the computed solids flux out of the riser. The simulated cases under different solids fluxes are listed in Table 3.

Fig. 7 displays time-averaged composition and the higher heating value for syngas out of the riser under various solids circulation fluxes from 260 to 1010 kg/m^{2}s. When the solids circulation flux increases from 260 to 480 kg/m^{2}s, the mole fraction of CO increases, which improves the quality of the syngas. With further increase of solids circulation flux from 480 to 600 kg/m^{2}s, the mole fractions of CO and H_2 fall down obviously, and the higher heating value of syngas decreases. As the solids flux is over 600 kg/m^{2}s, the quality of syngas changes little.

Table 3 Operating conditions under various solids circulation fluxes

Case	Solids circulation flux/kg·m^{-2}·s^{-1}
1	260
3	410
4	480
5	580
6	650
7	770
8	1010

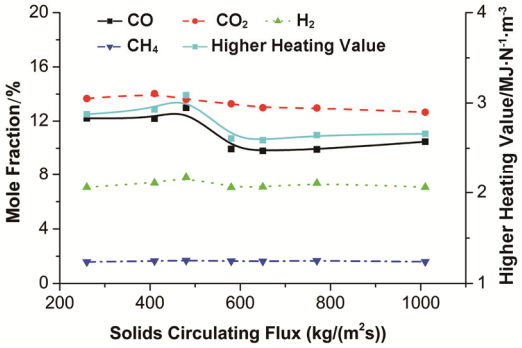

Fig. 7 Effect of solids circulation flux on the composition and higher heating value of syngas out of the riser

To illustrate how solids circulation flux affects the gasification performance, it is necessary to display more information about the gasification process under various solids fluxes. Fig. 8 and Fig. 9 display contours of the gas temperature and the solids volume fraction along the riser under different solids fluxes within 260-1010 kg/m^{2}s, respectively. Fig. 10 displays the time-averaged contours of gas mass fractions for three typical cases.

In the combustion zone, the mass fraction of CO rises while CO_2 descends with the solids flux increasing from 260 to 480 kg/m^{2}s as shown in Fig. 10. In the riser, particles carry heat from combustion zone at the bottom to the gasification zone in the upper region. When the solids flux increases, the solids concentration in the core of the riser rises, which enhances the gas-solid contact. It is helpful to improve the char combustion reaction, and more CO is produced in this region. When the solids flux increases to 480 kg/m^{2}s, more heat can be carried to the upper region, and the temperature becomes more uniform in the radial direction. And this promotes the gasification reactions, since the temperature distribution has great effect on chemical reactions [11]. The higher temperature

near the wall promotes the char heterogeneous gasification reactions, and the mass fraction of CO is uniform in the radial direction. Moreover, much more CO is produced in the combustion region, and the mole fraction of CO out of the riser increases. As discussed in the previous section, H_2O is released mostly from coal drying and pyrolysis, and about thirty percent H_2 is released from coal pyrolysis. Near the coal inlet, H_2O and H_2 are released quickly from coal pyrolysis under higher solids circulation flux due to higher temperature near the wall, thus the mass fractions of H_2O and H_2 near the coal inlet increase.

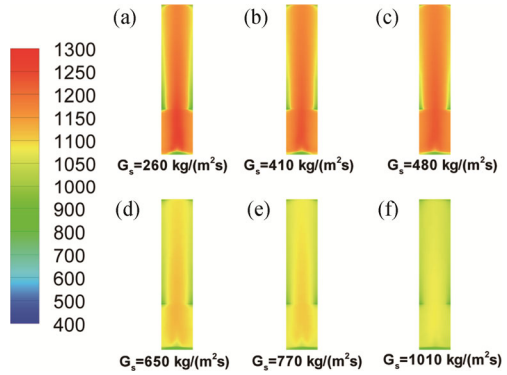

Fig. 8 Contours of gas temperature in the riser under different solids circulation fluxes

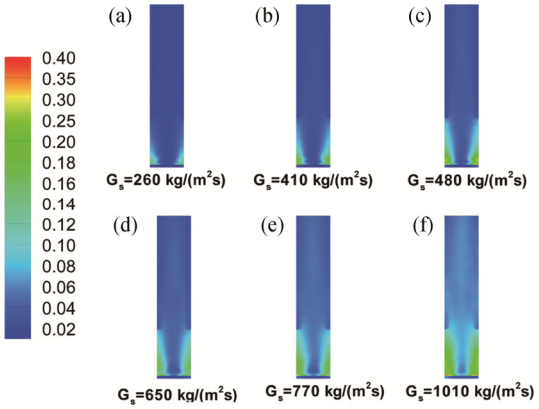

Fig. 9 Contours of solids volume fraction under different solids circulation fluxes

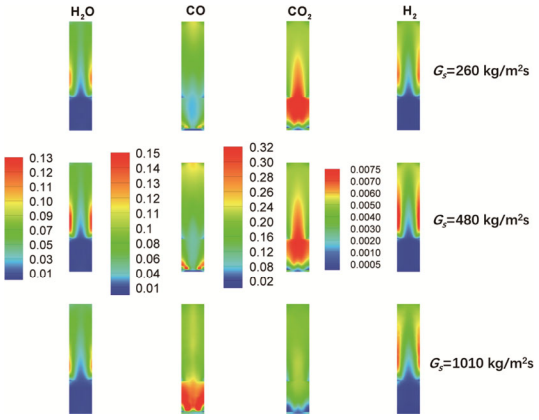

Fig. 10 Contours of gas mass fractions in the riser under different solids circulation fluxes

Further rise of solids circulation flux from 480 kg/m^{2}s makes the temperature in the combustion zone decrease obviously. The solids concentration in the riser increases under larger solids flux. As the other operating conditions keep the same, the produced heat from combustion zone will change little. The temperature rise of particles gets lower, and the temperature in the riser decreases. As shown in Fig. 8, the temperature all over the riser has a dramatic decrease from 480 to 650 kg/m^{2}s. The decrease of temperature inhibits the combustion reaction, and the converted carbon in the combustion zone decreases as the solids circulation flux increases. The decrease of temperature resulting from the increase of solids circulation flux slows the gasification reaction in the upper region. As a result, the mole fractions of CO and H_2 out of the riser decrease obviously.

In the CFB gasifier, the agglomeration problem should be avoided, thus the maximum temperature is an important indicator [11]. Fig. 11 shows the axial distributions of gas temperature at the core of the riser under various solids circulation fluxes from 260 to 1010 kg/m^{2}s. It can be found that the peak value of gaseous temperature in the combustion zone decreases when the solids circulation flux increases. As the solids flux increases beyond 600 kg/m^{2}s, the maximum temperature has a dramatic decrease, and the temperature in the gasification zone gets closer to that in the combustion zone. And this reveals that the distribution of temperature in the riser is more uniform under larger solids flux. High operating temperature is helpful to enhance the gasification reactions, thus large solids flux may reduce the gasification efficiency, although it can avoid agglomeration problem.

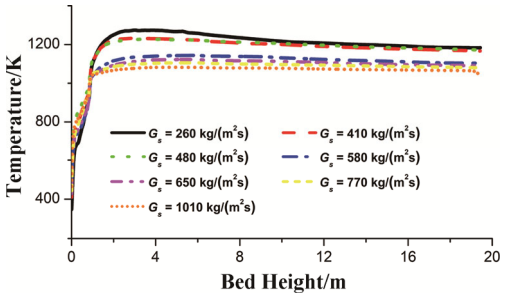

Fig. 11 The axial profiles of gas temperature in the core of the riser under different solids circulation fluxes

5. Conclusions

The CFD method has been developed to predict the

gasification process in pressurized high-density CFB gasifier and validated by two experimental cases. The coal gasification behavior under different solids circulation fluxes has been simulated. The predicted results revealed that the syngas quality reached the highest value around 480 kg/m^{2}s when the solids flux increased from 260 to 1010 kg/m^{2}s. To understand the effect of solids flux, the hydrodynamics characteristics and the distributions of gas species and temperature were further analyzed. The uniform solids concentration at 480 kg/m^{2}s distribution led to more uniform distribution of temperature in the axial and radial direction, which promoted both the char combustion and the gasification reactions in the riser. With further increase of solids flux, the temperature exiting the combustion zone decreased obviously, which inhibited the gasification process. The predicted results revealed that although high solids flux may avoid agglomeration due to the decrease of peak temperature, it might reduce the gasification efficiency and cause the operating difficulty; therefore an optimal solids flux should be chosen.

Acknowledgements

The authors gratefully acknowledge the financial support from National Science and Technology Major Project (No. 2015ZX07202-013) and National Natural Science Foundation of China (No. 91541123).

References

[1] Zhu J., Ma H., Liu D., Li J., Preheating characteristics of datong coal in O_2/CO_2 and air atmospheres. Journal of Thermal Science, 2018, 27(4): 341–348.

[2] Li T., Chaudhari K., VanEssendelft D., Turton R., Nicoletti P., Shahnam M., Guenther C., Computational fluid dynamic simulations of a pilot-scale transport coal gasifier: evaluation of reaction kinetics. Energy & Fuels, 2013, 27(12): 7896–7904.

[3] Singh R.I., Brink A., Hupa M., CFD modeling to study fluidized bed combustion and gasification. Applied Thermal Engineering, 2013, 52(2): 585–614.

[4] Zhang H., Zhang Y., Zhu Z., Lu Q., Circulating fluidized bed gasification of low rank coal: Influence of O_2/C molar ratio on gasification performance and sulphur transformation. Journal of Thermal Science, 2016, 25(4): 363–371.

[5] Cai C., Wu Y., Zhang J., Yue G., Lv J., Zhang H., Effects of the secondary oxygen injection on the performance of a staged-entrained flow coal gasifier. In: Qi H., Zhao B. (eds) Cleaner Combustion and Sustainable World. ISCC 2011. Springer, Berlin, Heidelberg, 2013, pp. 731–737.

[6] Wang S., Hydrodynamic characteristics in dense transport bed. PhD Dissertation, Institute of Engineering Thermophysics, Chinese Academy of Sciences, Beijing, China, 2012.

[7] Cau G., Tola V., Pettinau A., A steady state model for predicting performance of small-scale up-draft coal gasifiers. Fuel, 2015, 152: 3–12.

[8] Yu K.S., Experimental study on coal gasification process in dual circulating fluidized beds. Doctor, Graduate University of Chinese Academy of Sciences, Beijing, China, 2012.

[9] Li X.T., Grace J.R., Lim C.J., Watkinson A.P., Chen H.P., Kim J.R., Biomass gasification in a circulating fluidized bed. Biomass and Bioenergy, 2004, 26(2): 171–193.

[10] Zhang Y., Lei F., Wang S., Xu X., Xiao Y., A numerical study of gas–solid flow hydrodynamics in a riser under dense suspension upflow regime. Powder Technology, 2015, 280: 227–238.

[11] Shadle L.J., Monazam E.R., Swanson M.L., Coal gasification in a transport reactor. Industrial & Engineering Chemistry Research, 2001, 40(13): 2782–2792.

[12] Fang Y.T., Huang J.J., Wang Y., Zhang B.J., Experiment and mathematical modeling of a bench-scale circulating fluidized bed gasifier. Fuel Processing Technology, 2001, 69(1): 29–44.

[13] Kim Y.J., Lee J.M., Kim S.D., Modeling of coal gasification in an internally circulating fluidized bed reactor with draught tube. Fuel, 2000, 79(1): 69–77.

[14] Bi D., Guan Q., Xuan W., Zhang J. Numerical simulation of GSP gasifier under different swirl angles. Fuel, 2015, 155: 155–163.

[15] Adamczyk W.P., Kozołub P., Węcel G., Klimanek A., Białecki R.A., Czakiert T., Modeling oxy-fuel combustion in a 3D circulating fluidized bed using the hybrid Euler–Lagrange approach. Applied Thermal Engineering, 2014, 71(1): 266–275.

[16] Zhou H.S., Flamant G., Gauthier D., Lu J.D., Lagrangian approach for simulating the gas-particle flow structure in a circulating fluidized bed riser. International Journal of Multiphase Flow, 2002, 28(11): 1801–1821.

[17] Chu K.W., Yu A.B., Numerical simulation of complex particle–fluid flows. Powder Technology, 2008, 179(3): 104–114.

[18] Zhang Y., Ma Q., Xu X., Xiao Y., Lei F., Numerical study of gas–solid flow behavior in a two-stage high-density riser using EMMS-based drag model. Chemical Engineering and Processing: Process Intensification, 2015, 98: 71–85.

[19] Yang N., Wang W., Ge W., Li J., CFD simulation of concurrent-up gas–solid flow in circulating fluidized beds with structure-dependent drag coefficient. Chemical Engineering Journal, 2003, 96(1–3): 71–80.

[20] Lu X., Wang T., Water–gas shift modeling in coal

gasification in an entrained-flow gasifier. Part 1: Development of methodology and model calibration. Fuel, 2013, 108: 629–638.

[21] Wang S., Lu H., Liu G., Sheng Z., Xu P., Gidaspow D., Modeling of cluster structure-dependent drag with Eulerian approach for circulating fluidized beds. Powder Technology, 2011, 208(1): 98–110.

[22] Li T., Dietiker J.-F., Shadle L., Comparison of full-loop and riser-only simulations for a pilot-scale circulating fluidized bed riser. Chemical Engineering Science, 2014, 120: 10–21.

[23] Wang X.Y., Jiang F., Xu X., Fan B.G., Lei J., Xiao Y.H., Experiment and CFD simulation of gas–solid flow in the riser of dense fluidized bed at high gas velocity. Powder Technology, 2010, 199(3): 203–212.

[24] Zhang Y., Lei F., Xiao Y., The influence of pressure and temperature on gas-solid hydrodynamics for Geldart B particles in a high-density CFB riser. Powder Technology, 2018, 327: 17–28.

[25] Yu L., Lu J., Zhang X., Zhang S., Numerical simulation of the bubbling fluidized bed coal gasification by the kinetic theory of granular flow (KTGF). Fuel, 2007, 86(5–6): 722–734.

[26] Wang X., Jin B., Zhong W., Three-dimensional simulation of fluidized bed coal gasification. Chemical Engineering and Processing: Process Intensification, 2009, 48(2): 695–705.

[27] Armstrong L.M., Gu S., Luo K.H., Effects of limestone calcination on the gasification processes in a BFB coal gasifier. Chemical Engineering Journal, 2011, 168(2): 848–860.

[28] Armstrong L.M., Gu S., Luo K.H., Parametric study of gasification processes in a BFB coal gasifier. Industrial & Engineering Chemistry Research, 2011, 50(10): 5959–5974.

[29] Zhang Y., Lei F., Xiao Y., Computational fluid dynamics simulation and parametric study of coal gasification in a circulating fluidized bed reactor. Asia-Pacific Journal of Chemical Engineering, 2015, 10(2): 307–317.

[30] Xiao Y., Wang S., Yang S., Zhao K., Zeng X., Xu X., Solids acceleration length in a cold dense transport bed. Journal of Thermal Science, 2012, 21(6): 533–538.

[31] Wang C., Zhu J., Barghi S., Li C., Axial and radial development of solids holdup in a high flux/density gas–solids circulating fluidized bed. Chemical Engineering Science, 2014, 108: 233–243.

[32] Wang C., Zhu J., Li C., Barghi S., Detailed measurements of particle velocity and solids flux in a high density circulating fluidized bed riser. Chemical Engineering Science, 2014, 114: 9–20.

[33] Chang J., Zhang K., Zhu W., Yang Y., Gas–solid flow in a high-density circulating fluidized bed riser with Geldart group B particles. Particuology, 2016, 29: 103–109.

[34] Gunn D., Transfer of heat or mass to particles in fixed and fluidised beds. International Journal of. Heat and Mass Transfer, 1978, 21: 467– 476.

[35] Syamlal M., Bisset L., METC gasifier advanced simulation (MGAS) model. Morgantown Energy Technology Center: Morgantown, WV, 1992.
DOI: 10.2172/10127635

[36] Grant D.M., Pugmire R.J., Fletcher T.H., Kerstein A.R., Chemical model of coal devolatilization using percolation lattice statistics. Energy & Fuels, 1989, 3(2): 175– 186.

[37] Guenther C., Shahnam M., Syamlal M., Longanbach J., Cicero D., Smith P., CFD modeling of a transport gasifier. Proceedings of the 19th Annual Pittsburgh Coal Conference. Pittsburgh, Pennsylvania, 2002, pp. 24–26.